Q. Jl R. astr. Soc. (1987) **28**, 312–322

VARIATIONS IN ULTRAVIOLET EXTINCTION: EFFECT OF POLARIZATION REVISITED

J.Mayo Greenberg[1] *and Grzegorz Chlewicki*[2]

[1] Laboratory Astrophysics, University of Leiden, The Netherlands
[2] Laboratory for Space Research and Kapteyn Astronomical Institute, University of Groningen, The Netherlands

(Received 1987 February 28)

SUMMARY

The alignment of the particles responsible for the polarization and visual extinction is shown to provide a basis for changing the saturation level of the ultraviolet extinction without changing the particle sizes. If the particles are well aligned, it is predicted that there should be significantly lower extinction in the ultraviolet relative to the visible for stars viewed perpendicular to magnetic-field lines (maximum polarization) as compared with those viewed across the field lines. Preliminary evidence for such an effect is noted in Carina.

1 INTRODUCTION

The subject of this paper is one of those in which Dr Nandy has made some of his most significant contributions. In fact, one of the topics to be discussed provided the basis for the first scientific and ultimately personal interactions between one of us (J.M.G.) and Dr Nandy in the earliest phases of our respective work in astronomy.

In the early studies of interstellar extinction by the ubiquitous small solid particles in space, the term 'ultraviolet' was limited by the atmospheric absorption to observations in the wavelength range 3100–3700 Å. Many of the theoretical grain models for representing this extinction were based on the Mie theory of scattering by spheres, although it was known as early as 1949 (Hiltner 1949; Hall 1949) that the correlation of polarization with extinction (Hiltner 1956) must imply not only non-spherical but also aligned particles. Attention was only later directed to the idea that extinction by variously aligned but *identical* non-spherical particles could exhibit different shapes of extinction in the near ultraviolet (Greenberg 1960; Greenberg & Meltzer 1960). It was noted that elongated dielectric particles spinning about their short axes directed perpendicular to the line of sight would produce a wavelength dependence of extinction *as if* they were larger particles (larger interior wave phase shift in the sense of greater size to wavelength) spinning about axes along the line of sight. Because of the kind of magnetic alignment predicted by Davis & Greenstein (1951), the two situations corresponded (respectively) to the magnetic field being perpendicular to and along the line of sight. Accepting this line of reasoning and assuming that the galactic magnetic field followed the spiral arms, Greenberg & Meltzer suggested that the extinction of the stars in Perseus should show an earlier (smaller λ^{-1}) levelling off than those in Cygnus. Interestingly enough, Nandy (1964, 1965) observed that the slope of the ultraviolet part of the extinction curve in

Cygnus is higher than in Perseus. Did this confirm the prediction or was it due, as Nandy (1967) suggested, to different compositions of grains in Perseus and Cygnus?

Little further work on the correlation of polarization with variation in the ultraviolet extinction has been carried out. This was probably because of the excitingly new and unpredicted or *unpredictable* consequences of observations made above the Earth's atmosphere. It became evident that the apparent saturation at $\lambda^{-1} = 4\ \mu m^{-1}$ which had been suggested by ground-based measurements was misleading. A new structure – now identified as the 2200 Å hump (2175 Å, $4{\cdot}6\ \mu m^{-1}$) – was indicated (Stecher 1965). Satellite observations with *OAO2* (Bless & Savage 1970, 1972) not only confirmed and clarified the structure at about $4{\cdot}6\ \mu m^{-1}$ but showed that, following the subsequent dip in extinction at about $5{\cdot}8$–$6{\cdot}2\ \mu m^{-1}$, there was again a rise in the extinction as far as the instrument could detect. It is not the purpose of this paper to review all the ultraviolet extinction observations but, rather, to consider what possible effects varying alignment of those particles which produce the visual polarization may have on the absolute level of the extinction beyond $\lambda^{-1} \simeq 4\ \mu m^{-1}$; i.e. are there variations in the base level of the 2200 Å hump and of the far ultraviolet extinction?

2 THE TRIMODAL GRAIN DISTRIBUTION

In a series of papers (Greenberg & Chlewicki 1983; Chlewicki *et al.* 1984; Aiello *et al.* 1987), a thorough examination of the ultraviolet extinction curves for about 110 stars representing diffuse clouds has revealed several basic results: (1) At least 90 per cent exhibit a uniform *shape* in the FUV ($\lambda < 1800$ Å); (2) the correlation with visual extinction is far stronger for the hump (see Nandy *et al.* 1975) than for the FUV; (3) strong variations in the *amount* of FUV and, in some cases, in the hump occur systematically in some young OB associations. We emphasize here the high degree of uniformity of the shape in the region $5{\cdot}5 \simeq \lambda^{-1} \leqslant 8\ \mu m^{-1}$. Greenberg & Chlewicki (1983) concluded, as has been later confirmed by further observations and theoretical studies, that the grain populations producing the hump and the rise in extinction beyond the minimum must be distinct from each other as well as from the population producing the visible extinction. This is schematically illustrated in Fig. 1 where the saturation by the 'classical' particles (radii $\sim 0{\cdot}1\ \mu m$) occurs at about $\lambda^{-1} = 4\ \mu m^{-1}$ and where the hump and FUV contribution are *separately* added beyond this. We see then that varying the degree and direction of alignment would raise or lower both the entire regions of the hump and the FUV by raising or lowering the saturation as originally suggested *if* the particles responsible for the visible extinction were dielectric. There are a number of instances where such a variation in the saturation level is observed, but it remains to look for a correlation with the degree of polarization. One possibility is in the Carina complex where, as seen in Fig. 2, the level of both the hump and FUV extinction appears lower than the average, although their shapes are normal.

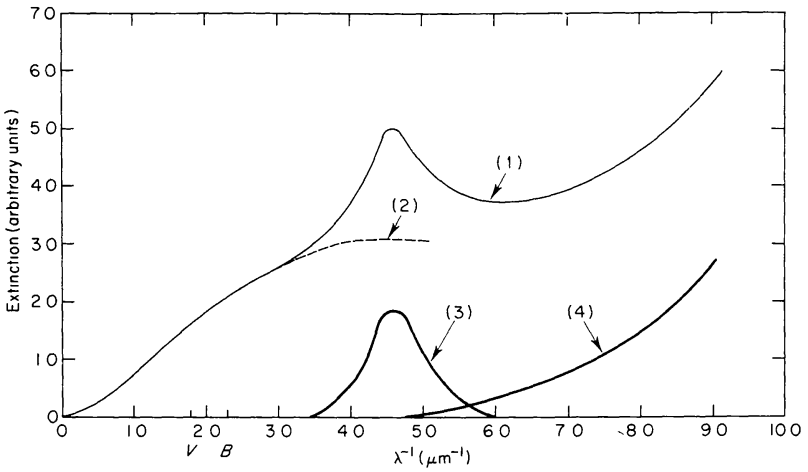

FIG. 1. Schematic representation of the mean extinction curve (1). The 'visual' portion (2) is the contribution made by classical size particles (radii ~ 0·1 μm). The hump (3) and the far-ultraviolet portion (4) are produced by much smaller particles.

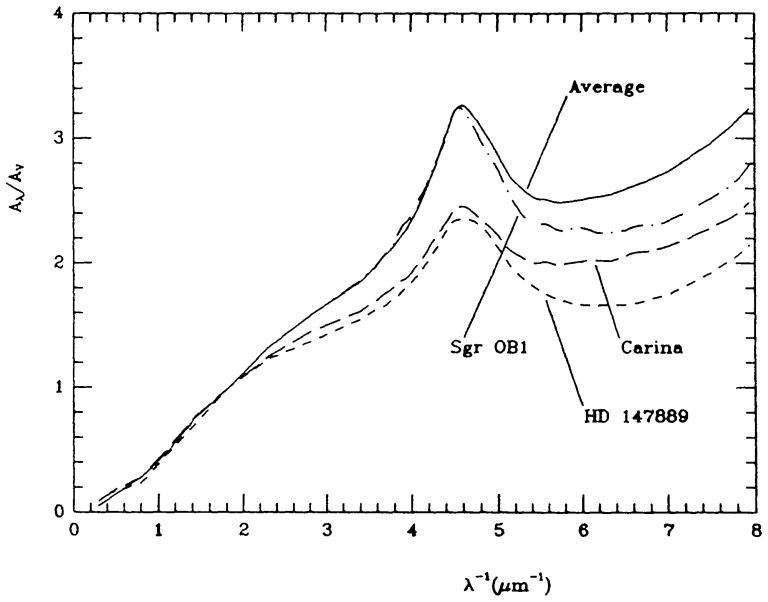

FIG. 2. Extinction curves for HD 147889 (in the Ophiuchus complex), an average of 7 stars near η Carinae and an average of 4 stars in Sgr OB1 compared with the average diffuse cloud extinction curve.

3 ALIGNMENT

It is generally agreed that magnetic torques are the primary cause of alignment. We shall restrict ourselves here to consideration of elongated particles and the calculations of extinction and polarization will be performed on the infinite cylinder representation. Ideal alignment is that in which the particles spin precisely about their short axes, which are lined up along the magnetic field. This we define as perfect spinning alignment (PSA). Davis–Greenstein alignment is more realistic in that it takes into account the misalignment produced by gas collisions (thermal spin-up) on the spinning

particle (Jones & Spitzer 1967; Greenberg 1968). Superthermal spin-up (hot-spots on the grains) was introduced by Purcell (1975) to enhance the Davis–Greenstein mechanism which has some difficulties with weak magnetic fields. These questions are discussed adequately elsewhere (Purcell 1979; Spitzer & McGlynn 1979; Aannestad & Greenberg 1983). For our purposes it is only necessary to recognize some of the consequences.

For Davis–Greenstein (D–G) alignment the spin axes are distributed over an angle β with respect to the magnetic field according to

$$f(\beta) = \frac{\xi \sin\beta}{(\xi^2 \cos^2\beta + \sin^2\beta)^{\frac{3}{2}}}, \tag{1}$$

normalized according to $\int_0^{\frac{1}{2}\pi} f(\beta)\, d\beta = 1$, where the alignment parameter ξ is given by

$$\xi^2 = \frac{a + \delta_0 T_d/T_g}{a + \delta_0} \tag{2}$$

and

$$\delta_0 = \left(\frac{\pi}{2 m_H k}\right)^{\frac{1}{2}} \frac{\chi''}{\omega} \frac{B^2}{n_H}, \tag{3}$$

where all terms are as defined in Hong & Greenberg (1980). The distribution function $f(\beta)$ for suprathermal alignment is a bit more complex (e.g. Purcell 1979; Aannestad & Greenberg 1983).

It may be shown that the reduction in the ratio of polarization to extinction (relative to PSA) is exactly given by equation (1) for small (Rayleigh size) particles and approximately, for particles with $2\pi a/\lambda \simeq 1$, by the Rayleigh reduction factor (Greenberg 1968)

$$\left.\begin{aligned} R^R &= \frac{(P/A)_{DG}}{(P/A)_{PSA}}, \\ &= \frac{3}{2(1-\xi^2)} - \frac{1}{2} - \frac{3\xi}{2} \frac{\sin^{-1}\sqrt{(1-\xi^2)}}{(1-\xi^2)^{\frac{3}{2}}}, \\ &= \tfrac{1}{2}[3\langle\cos^2\beta\rangle - 1]. \end{aligned}\right\} \tag{4}$$

A similar expression may be derived for the suprathermal spin-up alignment. The SSA alignment is overall more efficient than D–G and particularly so for smaller particles in the size distribution.

The extinction and polarization cross sections averaged over the distribution of spin angles are calculated from (Hong & Greenberg 1980)

$$Q_{ext} = \int_0^{\frac{1}{2}\pi} f(\beta)\, d\beta \frac{2}{\pi} \int_0^{\frac{1}{2}\pi} d\omega \frac{2}{\pi} \int_0^{\frac{1}{2}\pi} \tfrac{1}{2}\{Q_{ext}^E(\theta) + Q_{ext}^H(\theta)\}\, d\alpha, \tag{5}$$

$$Q_{pol} = \int_0^{\frac{1}{2}\pi} f(\beta)\, d\beta \frac{2}{\pi} \int_0^{\frac{1}{2}\pi} d\omega \frac{2}{\pi} \int_0^{\frac{1}{2}\pi} \tfrac{1}{2}\{Q_{ext}^E(\theta) - Q_{ext}^H(\theta)\} \cos 2\varphi\, d\alpha. \tag{6}$$

See Fig. 3 for the definitions of angles.

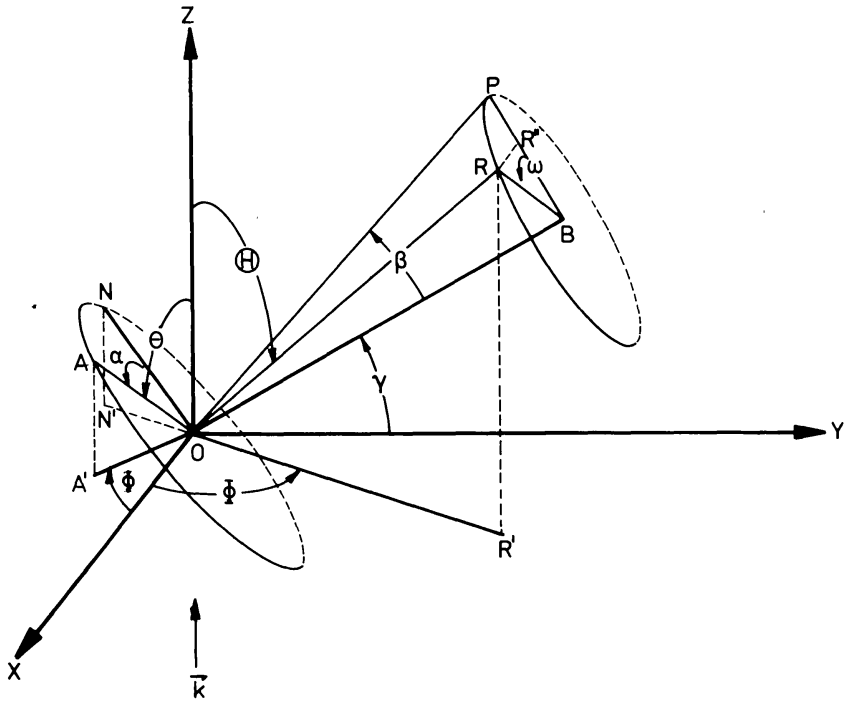

FIG. 3. Geometrical configuration of a wobbling grain: the coordinate origin is put at the grain centre O, the Z-axis is parallel to the direction of light propagation, $\mathbf{k}$; and the Y-axis is in the plane made by $\mathbf{k}$ and the particle alignment axis OB. The sky is represented by the XY-plane. The angle made by the alignment axis OB and Y-axis is the inclination angle, γ. The cylinder symmetry axis, OA, makes an angle θ with $\mathbf{k}$, and its projection on the sky plane makes an angle φ with the X-axis. The spin angle, precession angle and precession cone-angle are denoted, respectively, by α, ω and β. The spin angle is measured in the spinning plane, which is the extension of sector ONA.

Q_{sca} is calculated from a formula similar to (5). The imaginary part of (6) yields the amplitude of circular polarization, Q_{cir}.

The requirement of any alignment mechanism is that it should be able to produce at least a certain minimal polarization relative to extinction. This condition is not easily attained for the D–G mechanism using normal parameters for the interstellar medium. We shall choose $\delta_0 = 0{\cdot}215$ (Hong & Greenberg 1980) in order to give $P(V)/A(V) = 0{\cdot}03$.

4 NATURE OF THE POLARIZING PARTICLES

Mathis and colleagues (see Mathis 1986a; Mathis & Wallenhorst 1981 and references therein) attribute the polarization to silicate particles which provide only about one-third of the visible extinction. Greenberg and colleagues (see Greenberg 1985, 1986 and references therein) attribute the polarization to silicate core–organic refractory mantle particles which provide essentially the full visible extinction. It will probably turn out that, given the same ratio of polarization to extinction, the net effect on the ultraviolet of varying the direction of alignment in either model will be similar. However, we will limit ourselves here to the core–mantle grains because we feel that they are closer to the actual situation in space.

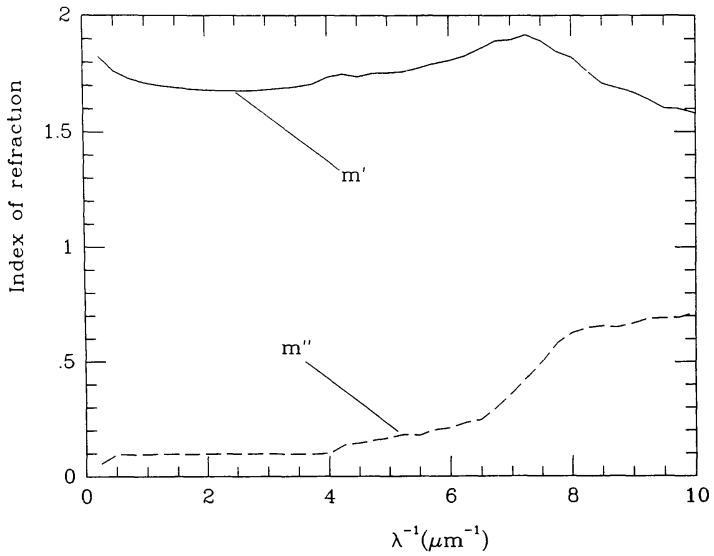

FIG. 4. Real (m') and imaginary (m'') parts of the index of refraction of the organic refractory mantle. The ultraviolet part is synthesized from 40 Lorentzians using the Clausius–Mosotti equation. The absorption in the visual is arbitrarily fixed and m' calculated from Kramers–Kronig relations.

The optical properties of the organic refractory mantle which dominates the core–mantle grain properties are represented here by assuming that it absorbs rather strongly in the ultraviolet and has a moderate absorption in the visual. The curve shown in Fig. 4 is taken as a rather extreme case of visual absorptivity. Details of the Kramers–Kronig programme and the choice of absorptivities will be published elsewhere.

The size distribution of core–mantle particles which reasonably fits the polarization maximum and the extinction is given by

$$n(a) = \exp\left[-5\left(\frac{a-a_c}{a_i}\right)^3\right], \tag{7}$$

where a_c = silicate core radius = 0·05 μm and a_i = 0.2 μm leading to a mean particle size $\langle a \rangle \simeq 0.11$ μm. This is rather smaller than one normally uses because our organic refractory is found to have a large value of $m' \geqslant 1{\cdot}6$ in the visual. A larger value of a_i (and of $\langle a \rangle$) would result from smaller values of m'', which by Kramers–Kronig give smaller m', as well as allowing m'' to decrease for longer wavelengths relative to that at V.

Mathis (1986a, b) has raised an objection to using the core–mantle particles for both polarization and extinction because he says that Martin's criterion (Martin 1972, 1974; Martin & Angel 1976) for the circular polarization reversal at the maximum of the linear polarization requires that the polarizing particles be dielectric (small absorptivity) and that such dielectric particles will have a much higher albedo than the observed one of $\alpha = 0.6$–0.7 (Savage & Mathis 1979). The answer to this objection is shown in Fig. 5. The albedos shown in the V-band for D–G and PSA are $\alpha \simeq 0{\cdot}7$ and $\alpha \simeq 0{\cdot}65$, respectively. Assuming that the particles responsible for the 2200 Å hump are absorbing in the visual and contributing about 10 per cent of the visual

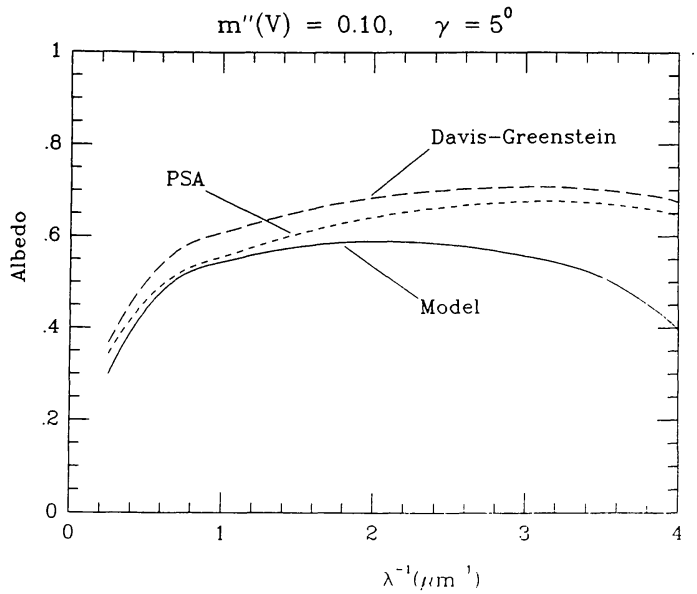

FIG. 5. Albedos (scattering/extinction) for PSA and D–G aligned cylindrical particles for $\gamma = 5°$ (see Fig. 3). The D–G albedo so defined is almost equal to the albedo for random alignment which is the 'normal' albedo. The model albedo includes a small component of small absorbing particles representing those responsible for the 220-nm hump.

extinction, the *net* albedo is brought down to $\alpha < 0{\cdot}6$, which is well within the limits prescribed by observations. Our calculations lead us to believe that values of m'' as low as 0·05 in the visual would also be satisfactory for the albedo criterion.

With regard to the circular polarization criterion, we had examined particles with values of m'' as high as 0·45 in the visual and found that even for these, the linear-circular polarization criterion is satisfied. This led us to look at the paper by Shapiro (1975) in which it was shown that the *highly absorbing* material, magnetite, was satisfactory. In fact, in that paper it was shown rather elegantly and simply that so long as the optical properties of the particles satisfy the *physically fundamental* Kramers–Kronig relations between $m'(\lambda)$ and $m''(\lambda)$ (as ours do) the polarization criterion is automatically satisfied even for m'' large. The linear polarization is, for aligned particles, proportional to a differential extinction in space and the circular polarization is proportional to a differential phase shift. They thus bear the same relationship with each other as the imaginary and real parts of the index of refraction of space, respectively (see, for example, Greenberg 1979). Just as the real part of an index of refraction shows anomalous dispersion in the region of an absorption, so the circular polarization is dispersive where the polarization is a maximum. Thus, it is not required that the polarizing particles be dielectric, *only* that they have physically *realistic* optical constants according to the Kramers–Kronig relations although with the proviso that the wavelength dependence of the linear polarization be acceptable.

For completeness we show in Fig. 6 how the circular polarization sign reversal occurs at the maximum in the linear polarization for both D–G and

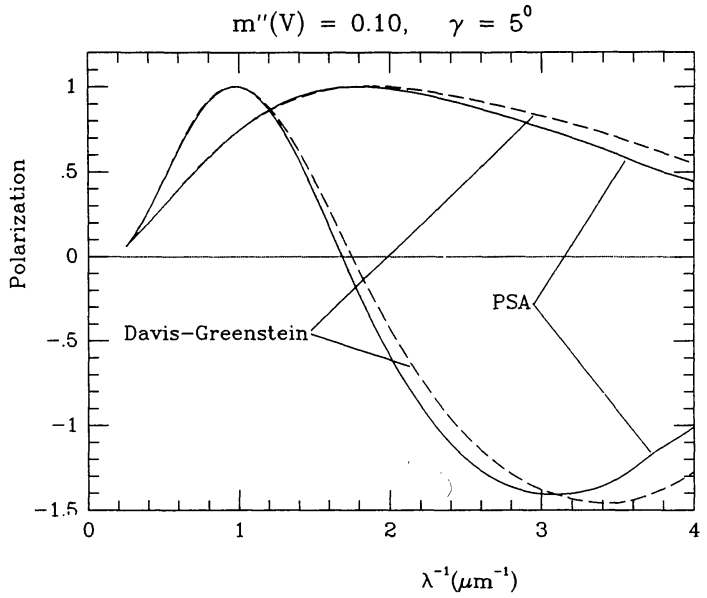

FIG. 6. Normalized linear and circular polarization for PSA and D–G aligned cylindrical particles for $\gamma = 5°$ (see Fig. 3).

PSA alignment. The angle between the line of sight and the magnetic field is 85° ($\lambda = 5°$), i.e. it displays almost perfect perpendicularity.

5 EFFECT OF ALIGNMENT ON ULTRAVIOLET EXTINCTION

The most extreme effect on the saturation extinction in the ultraviolet by the core–mantle particles occurs for PSA as shown in Fig. 7(a). The UV level decreases by as much as $\sim\frac{1}{3}$ depending on whether the line of sight is parallel or perpendicular to the magnetic field direction. With D–G alignment described by $P_{max}/A_v = 0{\cdot}03$ the effect is reduced to about 10 per cent [see Fig. 7b] which is significant but not as large as seen in Carina (Fig. 2). Actually, there is reason to expect that, locally, P_{max}/A_v must be substantially larger than 0·03 (Greenberg 1986) so that perhaps, qualitatively, the ultraviolet depression for high polarization may be better represented by the higher degree of alignment obtained for Purcell's mechanism [see Fig. 7(c)] where the maximum change is $\sim$ 20 per cent.

In Carina the FUV base level together with the hump base level are about 20 per cent lower than the average (see Fig. 2), although the *shape* of the FUV portion is quite normal. Such curves as those for HD 147889 and Sgr OB1 are quite different in that the curvature of the FUV is larger than average indicating a physical modification in the parameters of these particles

FIG. 7. Theoretical extinction curves for variously aligned cylindrical particles for magnetic fields at 85° ($\gamma = 5°$), 45°, 5° ($\gamma = 85°$) with respect to the line of sight. The optimum for polarization is B perpendicular to the line of sight ($\gamma = 0°$). (a) Perfect spinning alignment; (b) Davis–Greenstein alignment ($P_{max}/A_v = 0{\cdot}03$); (c) Suprathermal spin-up alignment ($P_{max}/A_v = 0{\cdot}075$).

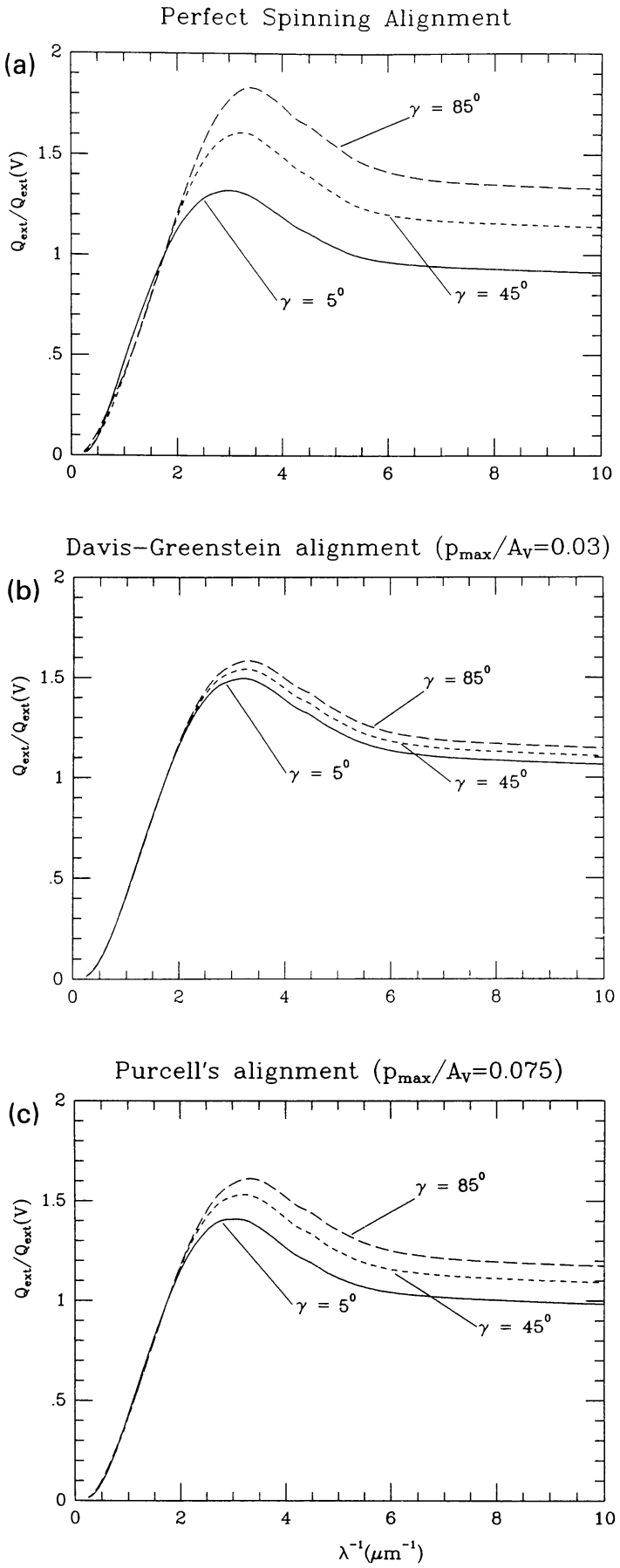

FIG. 7. For legend see opposite.

(Chlewicki *et al.* 1984). Polarimetry in B and V of about 60 stars belonging to the clusters Tr 14, Tr 16, and Coll 228 in the field of the Carina nebula shows a high degree of alignment of the polarization vectors indicating a highly ordered magnetic field; this may also imply a high degree of particle alignment (Marraco & Forte 1980). The ultraviolet extinction and the polarization in Carina thus appears to satisfy the correlation prediction.

We leave the question open at this time as to how strongly alignment affects ultraviolet extinction, but we believe that it is probably significant and should be included in comparison of grain model calculations.

6 CONCLUDING REMARKS

Evidence exists for variations in the base level for the extinction beyond $\lambda^{-1} = 4\ \mu m^{-1}$ which may be produced by variations in the degree of optical polarization. More observations of visual polarization are needed for those stars with well-established ultraviolet extinction curves in order to justify and quantify this correlation.

REFERENCES

Aannestad, P.A. & Greenberg, J.M., 1983. *Astrophys. J.*, **272**, 551.

Aiello, S., Barsella, B., Chlewicki, G., Greenberg, J.M., Patriarchi, P. & Perinotto, M., 1987. *Astr. Astrophys. Suppl.*, in press.

Bless, R.C. & Savage, B.D., 1970. In *Ultraviolet Stellar Spectra and Related Ground-Based Observations*, IAU Symp. No. 36, p. 28, eds Houziaux, L. & Butler, H.E., Reidel, Dordrecht, Holland.

Bless, R.C. & Savage, B.D., 1972. *Astrophys. J.*, **171**, 293.

Chlewicki, G., Greenberg, J.M., Aiello, S., Barsella, B., Patriarchi, P. & Perinotto, M., 1984. *Proc. 4th European IUE Conference*, **ESA SP-218,** p. 507.

Davis, L. & Greenstein, J.L., 1951. *Astrophys. J.*, **114**, 206.

Greenberg, J.M. 1960. *J. Applied Phys.*, **31**, 82.

Greenberg, J.M., 1968. In *Stars and Stellar Systems*, vol. 7, Nebulae and Interstellar Matter, p. 221, eds Middlehurst, B.M. & Aller, L.A., University of Chicago Press.

Greenberg, J.M., 1979. In *Infrared Astronomy*, p. 51, eds Setti, G. & Fazio, G.G., Reidel, Dordrecht, Holland.

Greenberg, J.M., 1985. In *Birth and Infancy of Stars*, p. 139, eds Lucas, R., Omont, A. & Stora, R., Elsevier.

Greenberg, J.M., 1986. In *Light on Dark Matter*, p. 177, ed. Israel, F.P., Reidel, Dordrecht, Holland.

Greenberg, J.M. & Chlewicki, G., 1983. *Astrophys. J.*, **272**, 563.

Greenberg, J.M. & Meltzer, A.S., 1960. *Astrophys. J.*, **132**, 667.

Hall, J.S., 1949. *Science*, **109**, 166.

Hiltner, W.A., 1949. *Science*, **109**, 165.

Hiltner, W.A. 1956. In *Vistas in Astronomy*, vol. 2, p. 1086, ed. Beer, A., Pergamon Press, Oxford.

Hong, S.S. & Greenberg, J.M., 1980. *Astr. Astrophys.*, **88**, 194.

Jones, R.V. & Spitzer, L. Jr., 1967. *Astrophys. J.*, **147**, 943.

Marraco, H.G. & Forte, J.C., 1980. In *Star Clusters*, IAU Symp. No. 85, p. 241, ed. Hesser, J.E., Reidel, Dordrecht, Holland.

Martin, P.G., 1972. *Mon. Not. R. astr. Soc.*, **159**, 179.

Martin, P.G., 1974. *Astrophys. J.*, **187**, 461.

Martin, P.G. & Angel, J.R.P., 1976. *Astrophys. J.*, **207**, 126.

Mathis, J.S., 1986a. In *Light on Dark Matter*, p. 171, ed. Israel, F.P., Reidel, Dordrecht, Holland.

Mathis, J.S., 1986b. *Astrophys. J.*, **308**, 281.

Mathis, J.S. & Wallenhorst, S.G., 1981. *Astrophys. J.*, **244**, 483.

Nandy, K., 1964. *Publ. R. Obs. Edin.*, **3**(6), p. 142.
Nandy, K., 1965. *Publ. R. Obs. Edin.*, **5**(2), p. 13.
Nandy, K., 1967. In *Interstellar Grains*, p. 17, eds Greenberg, J.M. & Roark, T.P., NASA SP-140.
Nandy, K., Thompson, G.I., Jamar, C., Monfils, A. & Wilson, R., 1975. *Astr. Astrophys.*, **44**, 195.
Purcell, E.M., 1975. In *The Dusty Universe*, p. 155, eds Field, G.B. & Cameron, A.G.W., Watson Publications.
Purcell, E.M., 1979. *Astrophys. J.*, **231**, 404.
Savage, B.D. & Mathis, J.S., 1979. *Ann. Rev. Astr. Astrophys.*, **17**, 73.
Shapiro, P.R., 1975. *Astrophys. J.*, **201**, 151.
Spitzer, L. Jr. & McGlynn, T.A., 1979. *Astrophys. J.*, **231**, 417.
Stecher, T.P., 1965. *Astrophys. J.*, **142**, 1683.